Intermediate Crack Debonding Model of FRP-Strengthened Concrete Beams Using XFEM

T. Mohammadi, B. Wan, and K. Harries

PhD. Candidate, Marquette University, Milwaukee, WI, USA, tayyebeh.mohammadi@mu.edu

Associate Professor, Marquette University, Milwaukee, WI, USA, baolin.wan@mu.edu

Associate Professor, University of Pittsburgh, Pittsburgh, PA, USA, kharries@pitt.edu

Abstract: The use of fiber reinforced polymer (FRP) systems as externally bonded reinforcement has become very popular for the repair and strengthening of reinforced concrete (RC) structures as an alternative to the traditional techniques. One of the common failure modes of FRP-strengthened concrete beams is intermediate crack (IC) debonding of the FRP initiated at the tip of flexural or flexural/shear cracks in the substrate concrete; locations at which the interface is subjected to mixed-mode loading. Because of the presence of the crack, conventional methods of modeling are inefficient; however, fracture mechanics criterion can be applied to analyze such a model. This study presents a numerical analysis method using the extended finite element method (XFEM) implemented in Abaqus to model FRP intermediate crack debonding failure started at the tip of a flexural crack in a plain concrete beam specimen. XFEM models a crack as an enriched feature by adding degrees of freedom in elements with special displacement functions and does not require the mesh to match the geometry of the discontinuities. It can be used to simulate initiation and propagation of a discrete crack by using fracture energy criterion along an arbitrary, solution-dependent path without the requirement of remeshing. The numerical results are validated against experimental data demonstrating good agreement between them.

Keywords: Concrete Beam, Debonding Failure, Flexural Crack, FRP, XFEM

1. Introduction

Fiber reinforced polymer (FRP) are composite materials comprised of high strength fibers embedded in a polymer matrix. The result is a rigid material that has high strength and stiffness yet light weight. The fibers provide the stiffness and strength of the composite in the direction of their primary orientation while the polymer holds the fibers in alignment, transfers loads between fibers and serves to protect the fibers from mechanical and environmental damage.

Externally bonded FRP plate/sheet applied to the tension face of concrete beams or slabs for flexural repair/strengthening are widely used in civil engineering (Bakis, 2002; Oehlers, 2004) due to good material properties of FRP for this application. The main advantages of FRPs are their very high strength- and stiffness-to-weight ratios, corrosion resistance, and ease of installation compared to traditional techniques (ACI 440.2R, 2008). Along with these advantages, the use of externally bonded FRP plates/sheets introduces a new and unique mode of failure in strengthened structures. Failure of FRP-strengthened reinforced concrete beams dominated by flexure is often caused by debonding of the FRP layer along with a thin layer of concrete paste (Aprile, 2001;

Buyukozturk, 2004); this is a sudden and brittle failure. FRP debonding along the FRP–concrete interface can be categorized into two main categories (Teng, 2003): (a) plate-end (PE) debonding which initiates at the end of the FRP plate and propagates in the direction of increasing moment results from the high interface stresses at end discontinuities, and (b) intermediate crack-induced (IC) debonding which initiates in the beam span at a flexural or shear/flexural crack in the concrete and propagates towards the plate end in the direction of decreasing moment as shown schematically in Figure 1. This type of FRP debonding failure, unlike PE debonding that can be mitigated using anchorage at the plate end, is difficult to prevent. Thus, it should be taken into consideration in the design process and addressed as a limit state. The FRP/concrete interface at the tip of the flexural/shear cracks is subjected to mixed-mode loading conditions (Wan, 2004; Dai, 2009) consisting of a Mode I force component perpendicular to the interface due to shear force in the beam span and a Mode II force along the interface due to tension in the FRP induced by bending moment acting on the beam. These Mode I and II forces at the location of a crack are shown in Figure1. For the proper modeling of IC debonding, mixed-mode loading conditions must be considered. In the present paper, experiments conducted by (Harries, 2012) are studied using the extended finite element method (XFEM) in order to validate the applied method to model IC debonding failure of FRP-strengthened beams. XFEM is able to model cracks through the elements under mixed-mode loading conditions using traction separation laws.

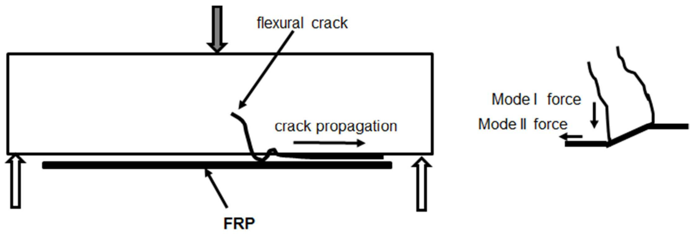

Figure 1. Typical intermediate crack (IC) debonding failure.

2. Experimental background

A variety of test methods have been used to describe FRP-to-concrete bond characteristics. Proposed methods may be categorized into two fundamental forms: pull-off tests (essentially pure Mode II loading) and beam flexure tests. The beam tests better represent actual in situ behavior in concrete structures as they capture the desired mixed-mode behavior. A practical standardized beam test method for assessing FRP-to-concrete bond behavior in FRP-strengthened beams was proposed by (Harries, 2012) and is presently being developed by ASTM Committee D30-plastics.The notched three-point bending beam specimen, shown in Figure 2, used for standardization is similar to that used to determine the modulus of rupture of concrete (ASTM C78). To capture the FRP debonding behavior, the beam is notched at midspan to one half of the beam depth to model cracked concrete. Nine specimens reported by (Harries, 2012) are considered in this study – three repetitions of three specimen details presented in Table 1. In the table, t_{FRP} is the thickness of glass fiber FRP (GFRP) plate used. These specimens are used to validate the proposed methods in the analysis.

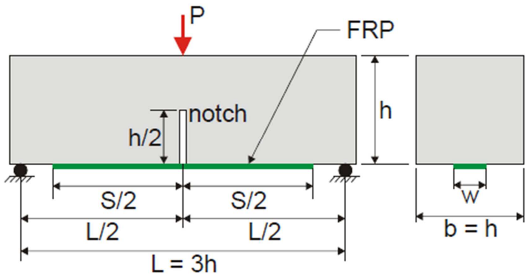

Figure 2. Test specimen (Harries, 2012).

Table 1. Specimen details.

Specimens	h=b=L/3 (mm)	w (mm)	t_{FRP} (mm)	S (mm)
G1-A, B and C	152	25	1.9	380
G2-A, B and C	152	50	1.9	380
G3-A, B and C	152	75	1.9	380

3. FRP debonding modeling using XFEM

As discussed previously, the FRP/concrete interface in FRP-strengthened concrete members is subjected to mixed-mode loading conditions. Therefore, the finite element analysis method should be able to simulate the behaviors of FRP debonding from concrete when the interface is subjected to mixed-mode loading. XFEM technique has been used in this study to investigate its ability to model this FRP/concrete interface debonding failure.

The extended finite element model (XFEM) was first proposed in the context of fracture by (Belytschko, 1999). XFEM allows the presence of discontinuities (cracks) in the elements of a finite element analysis by enriching the element with additional degrees of freedom. This technique can model crack opening and increase the accuracy of the approximation near the crack tip. The degree of freedom enrichment is done with special displacement functions as shown in Equation 1.

$$u = \sum_{i} N_i(x) \left[u_i + a_i H(x) + \sum_{j=1}^{4} b_i^j F_j(x) \right] \quad (1)$$

where $N_i(x)$ are the usual nodal shape functions; u_i are the usual nodal displacements; a_i are enrichment degrees of freedom associated with crack separation away from the tip; *H(x)* is the associated discontinuous jump function across the crack; b_i^j are the nodal enriched degrees of freedom associated with near-tip displacement; and $F_j(x)$ are the asymptotic crack tip functions given by:

$$F_j(x) = \left[\sqrt{r}\sin\frac{\theta}{2}, \sqrt{r}\cos\frac{\theta}{2}, \sqrt{r}\sin\frac{\theta}{2}\sin\theta, \sqrt{r}\cos\frac{\theta}{2}\cos\theta\right] \quad (2)$$

where r and θ are the polar coordinates from the crack tip. In Equation 1, the first term on the right-hand side is valid for all nodes in the model; the second term is used for nodes whose shape function is cut by the crack interior (the part between the old and new crack tips); and the third term is applicable only for nodes whose shape function is cut by the new crack tip.

Modeling the crack tip singularity accurately requires continuously keeping track of where the crack propagates. It is difficult because the degree of crack singularity depends upon the location of the crack in a non-isotropic material. One alternative approach within the framework of XFEM is based on traction-separation cohesive behavior (Abaqus, 6.11). Unlike cohesive surface methods, which need to have predefined paths align with element boundaries for the crack propagation, the XFEM can model crack initiation and propagation along an arbitrary, solution-dependent path in the bulk material, and crack propagation is not tied to the element boundaries in a mesh. In this case, the asymptotic near-tip singularity is ignored, and only the discontinuous jump across a cracked element is considered.

The failure mechanism including the degradation and the eventual separation between the two surfaces consists of two components: a damage initiation criterion and a damage evolution law. In this study, a bilinear traction separation law is assumed to model the bond behavior of the interface as shown in Figure 3. In the bilinear law, the initial response is the ascending linear branch, and the damage follows the descending linear branch once the damage criterion is met. A scalar damage variable, *D*, represents the overall damage at the contact point which has an initial value of 0. When the damage evolution is started, *D* monotonically evolves from 0 to 1 upon continued loading after the initiation of damage (Abaqus, 6.11). According to Figure 3, the contact tractions are affected by the damage as follows:

$$t = (1 - D)K_0\delta \quad (3)$$

The damage initiates when the contact stresses and/or contact separations satisfy the damage initiation criterion. For the present study, an elliptic form, Equation. 4, is considered as the damage initiation criterion:

$$\left(\frac{\sigma}{\sigma_n}\right)^2 + \left(\frac{\tau}{\tau_s}\right)^2 = 1 \quad (4)$$

where σ_n, and τ_s are the normal and shear bond strengths of the interface, respectively; and σ and τ are the normal and shear stresses of the element under mixed-mode loading, respectively.

The damage evolution law describes the rate at which the cohesive stiffness is degraded after the initiation criterion has been reached. It has been proposed by several researchers (Wan, 2004; Dai, 2009) that the relationship between the critical strain energy release rate components $\boldsymbol{G_{IC}}$ and $\boldsymbol{G_{IIC}}$ is linear. Therefore, a linear fracture criterion for mixed-mode loading has been used:

$$\frac{G}{G_C} = \left(\frac{G_I}{G_{IC}}\right) + \left(\frac{G_{II}}{G_{IIC}}\right) = 1 \tag{5}$$

where G_I and G_{II} are the strain energy release rate components of Mode I and II, respectively; and G_{IC} and G_{IIC} are the critical strain energy release rates in pure Mode I and Mode II loadings, respectively.

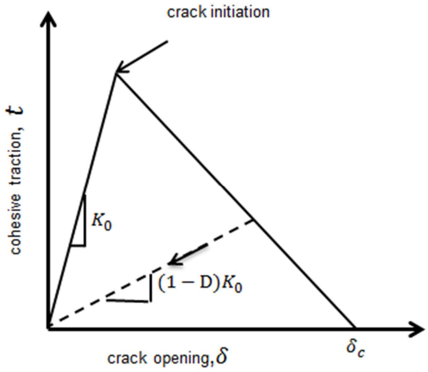

Figure 3. Bilinear traction separation law.

Figure 4 is a schematic representation of the dependence of damage initiation and evolution on the mixed-mode for a traction-separation response. The figure shows the traction on the vertical axis and the magnitudes of the normal and shear separations along the two horizontal axes. The unshaded triangles in the vertical coordinate planes represent the responses under the pure normal and shear separations (i.e.: Figure 3), respectively. The shaded vertical planes A and B represent the damage responses in Mode I and Mode II under mixed-mode conditions, respectively. The shaded triangle C shows the bond behavior of the interface under mixed-mode loading.

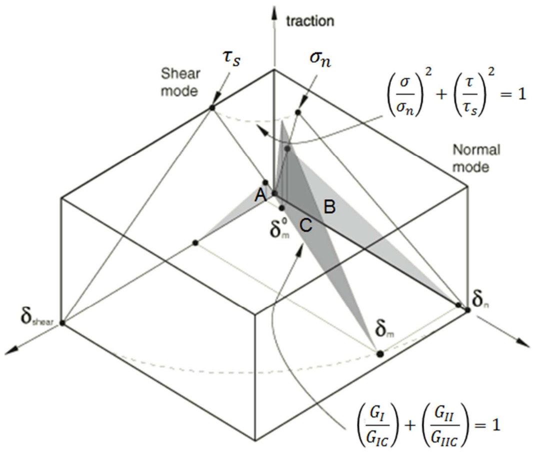

Figure 4. Mixed-mode response in cohesive interactions (Abaqus user's manual).

4. Finite element analysis

The finite element analysis software Abaqus/Standard was used in this research for the numerical analysis. The plane strain element (CPE4R) was applied to build the model. The typical specimen mesh of the model is shown in Figure 5. In XFEM, it is required to define a domain region through which the crack would probably propagate. Typically, experimental observations indicate that FRP debonding propagates through the concrete immediately adjacent to the concrete/adhesive interface (Wan, 2004). Therefore, a damaged area (crack domain) was created in the FE model to simulate the concrete close to the FRP/concrete interface. The traction separation law was assigned to this area using Equations 4 and 5.

Concrete material was modeled using the concrete damaged plasticity model. This model can describe the nonlinear behavior of concrete including failures in both tension and compression (Lubliner, 1989). The behaviors of FRP and epoxy adhesive were modeled by a brittle cracking model. The material properties of the substrate concrete, GFRP plate, and adhesive used in the FE analysis are presented in Table 2. Also, the required crack domain properties (debonding properties) of the specimens are shown in Table 3.

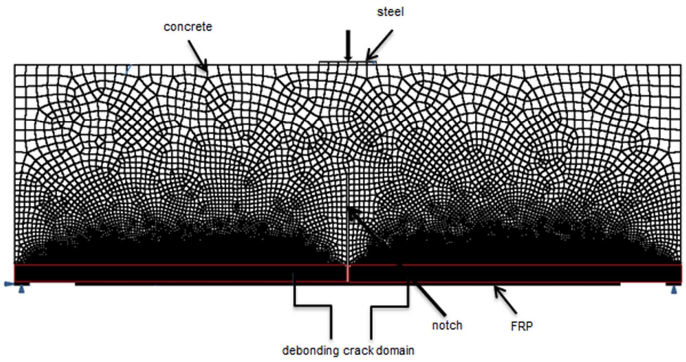

Figure 5. The typical finite element mesh.

Table 2. Material properties used in XFEM (Harries, 2012).

Material Property	Concrete	GFRP	Adhesive
Young Modulus, E,(GPa)	26.1	41.37	1.2
Compressive Strength, f_c', (MPa)	32	-	-
Tensile Strength, f_t', (MPa)	3.5	-	-
Poison Ratio,v	0.25	0.2	0.3
Fracture Energy, G_F, (N/m)	100	-	-

Table 3. Debonding properties used in XFEM.

Debonding property	15-G1	15-G2	15-G3
Young Modulus, E,(GPa)	26.1	26.1	26.1
Normal Strength, σ_n, (MPa)	3.5	3.5	3.5
Shear Strength, τ_s, (MPa)	1.54	1	0.9
Fracture Energy Mode I, G_F, (N/m)	150	150	150
Fracture Energy Mode II, G_F, (N/m)	200	180	170

5. Results

Figure 6 shows the load vs. FRP strain curves (recorded immediately below the vertical notch) of experimental data from the concrete specimens tested by (Harries, 2012) and the numerical results from the present analyses. There are three identical specimens A, B, and C in each set – these indicate the variation typical of this test. It can be seen in Figure 6 that the XFEM method is able to predict the trends of specimen behaviors and debonding failure. Generally, the numerical analysis has given stiffer results compared with experimental results; this is typical when modeling concrete structures.

Based on the experimental observations, the FRP debonding failure propagates through the concrete immediately adjacent to the FRP/concrete interface. This phenomenon can be seen in the numerical analysis too. Figure 7 presents the crack initiation and debonding failure propagation obtained from numerical analysis for specimen G1. The debonding starts in the first element of the damaged band adjacent the concrete/FRP interface at the tip of notch (Figure 7-a). As element stresses meet the initiation criterion (Equation 4), the crack propagates toward the support (Figure 7-b).

6. Conclusion

In this research, finite element analysis was successfully conducted using XFEM to model FRP/concrete interface debonding in flexurally-strengthened plain concrete beams. The debonding initiation and propagation criteria were assigned to a crack domain during numerical simulation in order to model debonding failure. Numerical results were validated against experimental observations. Numerical analysis predicted that the crack initiated and propagated in the concrete layer close to the FRP/concrete interface which is consistent with experimental observation. Thus, this method is able to predict debonding failures of the FRP/concrete interface undergoing mixed-mode loading conditions.

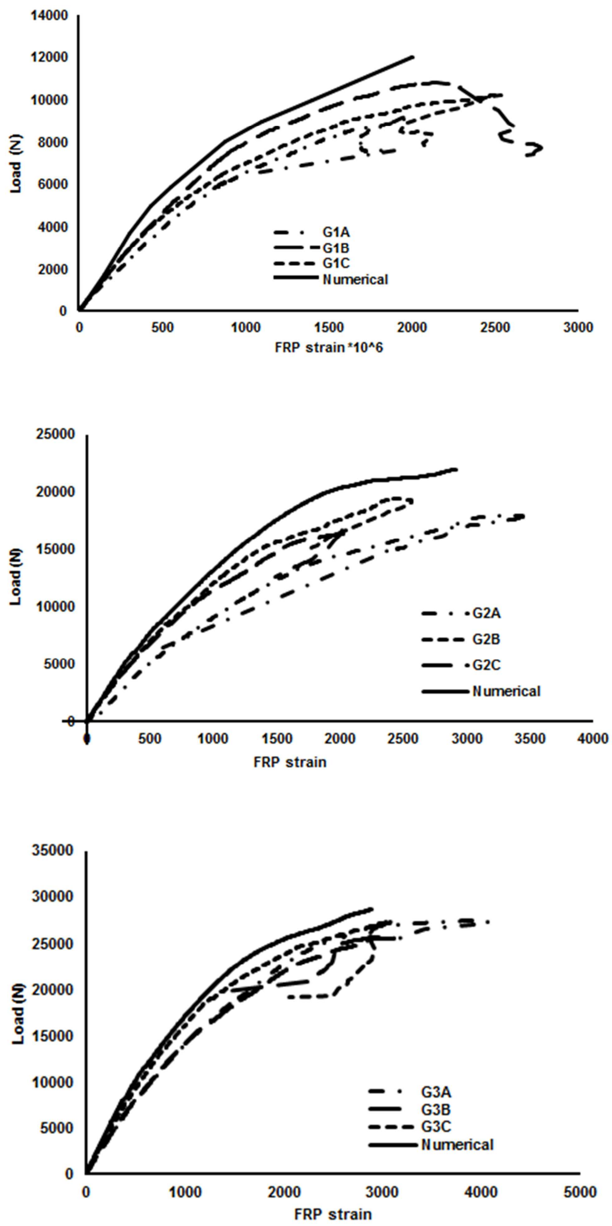

Figure 6. Experimental and numerical load vs. FRP strain curves.

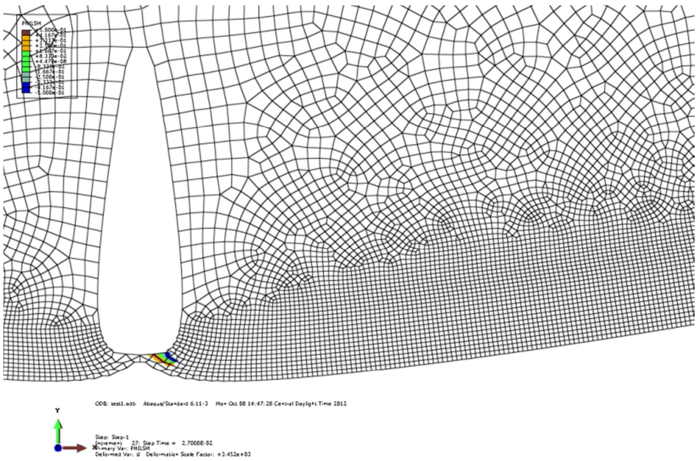

(a)

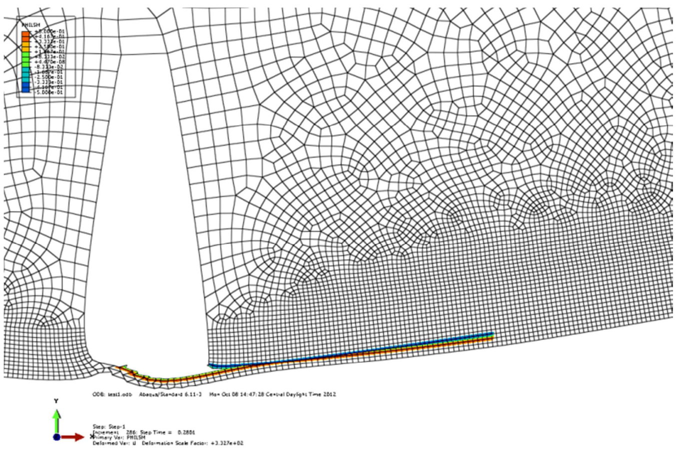

(b)

Figure 7. (a) Crack initiation, (b) crack propagation.

7. References

Abaqus/Standard User's Manual, Version 6.11. Dassault Systémes Simulia Corp., Providence, RI.

ACI 440.2R-08, "Guide for the Design and Construction of Externally Bonded FRP Systems for Strengthening Concrete Structures", Reported by ACI Committee 440, 2008.

American Society for Testing and Materials (ASTM) C78-10, "Standard Test Method for the Flexural Strength of Concrete (Using Simple Beam with Third Point Loading)," West Conshohocken, PA.

Aprile, A., Spacone, E., and Limkatanyu, S., "Role of Bond in RC Beams Strengthened with Steel and FRP Plates," Journal of Structural Engineering, 127(12), 2001.

Bakis, C.E., Bank, L.C., Brown, V.L., Cosenza E, Davalos J.F., and Lesko, J.J., " Fiber Reinforced Polymer Composites for Construction State-of-the Art Review," Journal of Composites for Construction, 6(2), 2002.

Belytschko, T., and Black, T., "Elastic Crack Growth in Finite Elements with Minimal Remeshing," International Journal for Numerical Methods in Engineering, 45, 1999.

Buyukozturk, O., Gunes, O.,and Karaca, E., "Progress on Understanding Debonding Problems in Reinforced Concrete and Steel Members Strengthened Using FRP Composites," Construction and Building Materials,18(1), 2004.

Dai, J., Wan, B., Yokota, H., and Ueda,T., "Fracture Criterion for Carbon Fiber Reinforced Polymer Sheet to Concrete Interface Subjected to Coupled Pull-out and Push-off Actions," Advances in Structural Engineering, 12, 2009.

Harries, K., Hamilton, H.R., Kasan, J., and Tatar, J., "Development of Standard Bond Capacity Test for FRP Bonded to Concrete," 6th international conference on Fiber Reinforced Polymer (FRP) Composites in Civil Engineering (CICE), 2012.

Lubliner, J., Oliver, J., Oller, S., and Onate E., "Plastic-Damage model for Concrete", International Journal of Solid Structures, 25,1989.

Oehlers, D.J., and Seracino, R.," Design of FRP and Steel Plated RC Structures: Retrofitting Beams and Slabs for Strength, Stiffness and Ductility," UK, Elsevier; 2004.

Teng, J.G., Smith, S.T., Yao, J., and Chen, J.F "Intermediate Crack-Induced Debonding in RC Beams and Slabs," Construction and Building Materials,17(6-7), 2003.

Wan, B., Sutton, M.A., Petrou, M.F., Harries, K., and Li, N.,''Investigation of Bond Between Fiber Reinforced Polymer and Concrete Undergoing Global Mixed-mode I/II Loading", Journal of Engineering Mechanics, 103, 2004.